

Published in final edited form as:

Gastroenterology. 2013 March ; 144(3): . doi:10.1053/j.gastro.2012.11.022.

Weight-Independent Effects of Roux-en-Y Gastric Bypass on Glucose Homeostasis via Melanocortin-4 Receptors in Mice and Humans

Juliet F. Zechner^{1,2}, Uyenlinh L. Mirshahi⁶, Santhosh Satapati^{1,3}, Eric D. Berglund^{1,2}, Jari Rossi⁴, Michael M. Scott⁵, Christopher D. Still⁶, Glenn S. Gerhard⁶, Shawn C. Burgess^{1,3}, Tooraj Mirshahi⁶, and Vincent Aguirre^{1,2,*}

¹UT Southwestern Medical Center, Dallas, TX 75390, USA ²Center for Hypothalamic Research, Department of Medicine ³Advanced Imaging Center, Department of Pharmacology ⁴Institute of Biomedicine, Anatomy, University of Helsinki, Helsinki, Finland ⁵Department of Pharmacology, University of Virginia, Charlottesville, VA 22903, USA ⁶Weis Center for Research and Geisinger Obesity Research Institute, Geisinger Clinic, Danville, PA 17822, USA

Abstract

Background & Aims—Roux-en-Y gastric bypass (RYGB) improves glucose homeostasis independently of changes in body weight by unknown mechanisms. Melanocortin-4 receptors (MC4R) have weight-independent effects on glucose homeostasis, via autonomic neurons, and might also contribute to weight loss after RYGB. We investigated whether MC4Rs mediate effects of RYGB, such as its weight-independent effects on glucose homeostasis, in mice and humans.

Methods—We studied C57BL/6 mice with diet-induced obesity, MC4R-deficient mice, and mice that re-express MC4R specifically in autonomic neurons after RYGB or Sham operations. We also sequenced the *MC4R* locus in patients undergoing RYGB, to investigate diabetes resolution in carriers of rare *MC4R* variants.

Results—MC4Rs in autonomic brainstem neurons (including the parasympathetic dorsal motor vagus) mediated improved glucose homeostasis independent of changes in body weight. In contrast, MC4Rs in cholinergic preganglionic motor neurons (sympathetic and parasympathetic) mediated RYGB-induced increased energy expenditure and weight loss. Increased energy expenditure after RYGB is the predominant mechanism of weight loss and confers resistance to weight gain from a high-fat diet, effects of which are MC4R-dependent. MC4R-dependent effects of RYGB still occurred in mice with *Mc4r* haplosufficiency, and early-stage diabetes resolved at a similar rate in patients with rare variants of *MC4R* and non-carriers. However, carriers of *MC4R* (I251L), a rare variant associated with increased weight loss after RYGB and increased basal activity in vitro, were more likely to have early and weight-independent resolution of diabetes than non-carriers, indicating a role for MC4Rs in the effects of RYGB.

Conclusions—MC4Rs in autonomic neurons mediate beneficial effects of RYGB, including weight-independent improved glucose homeostasis, in mice and humans.

*Correspondence: Vincent Aguirre, UT Southwestern Medical Center, 5323 Harry Hines Blvd, Dallas, TX 75390, Phone: 214-648-0201, Fax: 214-648-5612, Vincent.Aguirre@UTSouthwestern.edu.

The authors declare no conflicts of interest.

Author Contributions: JFZ, ULM, SS, EDB, SCB, TM, and VA (study design and execution); JR and MS (animals); CDS and GSG (human samples); VA (drafted manuscript); JFZ, EDB, SCB, TM, and VA (critical revision).

Keywords

weight-loss surgery; stomach; mouse model; insulin sensitivity

Introduction

Fasting glycemia often improves within days of Roux-en-Y gastric bypass (RYGB) and RYGB provides greater improvements in glucose homeostasis than equivalent weight loss from calorie restriction or restrictive bariatric procedures.¹⁻³ This suggests that neurohormonal pathways provide additional, weight-independent mechanisms of improved gluco-regulation after RYGB, prompting intensive pre-clinical investigation of these mechanisms.

RYGB reduces body weight in mice,⁴ and a recent study by Hatoum, et.al,⁵ suggests that melanocortin-4 receptors (MC4R) are required for this effect. MC4Rs play a critical role in body weight regulation as evidenced by severe obesity in humans with naturally-occurring mutations and *Mc4r*-deficient mice.⁶⁻⁸ MC4Rs are expressed in the hypothalamus and hindbrain⁹⁻¹² and function broadly to reduce energy intake and increase expenditure in response to peripheral signals of energy excess, including gut hormones.¹³ MC4Rs are also expressed in autonomic neurons including cholinergic preganglionic motor neurons (sympathetic and parasympathetic)^{9-12, 14} and parasympathetic vagal sensory neurons.^{15, 16} Thus, MC4Rs provides a mechanistic link between the gut, central nervous system, and autonomic output to the abdominal viscera and brown adipose. However, studies, including the aforementioned from Hatoum et.al, suggest that MC4R is not involved during RYGB as human carriers of non-synonymous *MC4R* coding variants, which occur in 1-6% of severely obese patients,¹⁷ exhibit the expected weight loss after RYGB.^{5, 18} In apparent contrast to this data, Hatoum et al., conclude that MC4R is required during RYGB based on the failure of RYGB-treated MC4R-deficient mice to exhibit a statistically-significant weight reduction compared to Sham-operated mice. However, this conclusion is based on an experiment involving three animals per experimental group and 40% surgical mortality, introducing substantial possibility of type 2 error and survival bias. A definitive conclusion regarding the requirement of MC4R during RYGB is therefore precluded and the role of MC4R during RYGB remains unclear.

Herein, we investigate the contribution of MC4Rs to effects of RYGB using C57BL/6 mice with diet-induced obesity (DIO), MC4R-deficient mice, and mice with tissue-selective expression of MC4R exclusively in autonomic neurons. We also examine effects of RYGB on diabetes resolution in carriers of rare *MC4R* variants, including carriers of *MC4R*(I251L), a variant previously associated with enhanced RYGB-induced weight loss.¹⁹ We find that MC4Rs in autonomic neurons mediate beneficial effects of RYGB including weight-independent improved glucose homeostasis in mice and humans.

Results

RYGB increases energy expenditure to induce weight loss in DIO mice

RYGB reduced body weight of DIO mice by 27% compared to Sham operations (Figure 1A); fat mass was reduced by 65% and lean mass by 11% (Figure 1B). RYGB did not reduce intake (Figure 1C) or increase physical activity (Supplemental Figure 1A). Instead, it reduced feeding efficiency by 52% (Figure 1D), which was due to a 33% increase in energy expenditure (Figure 1E). While calorie absorption was reduced slightly after RYGB, feeding efficiency was still reduced by 46% after adjusting for these losses (Figure 1D, F), demonstrating that increased energy expenditure was the predominant mechanism of weight

loss. Daily calorie restriction of 27% was required to match the body weights of a separate group of sham-operated mice to RYGB mice [calorie-restricted, weight-matched sham (CRWM-Sham)] (Figure 1, A-C). Fasting plasma leptin was comparably reduced in RYGB and CRWM-Sham mice (Supplemental Figure 1B).

RYGB improves hepatic glucose homeostasis in DIO mice

Glucose homeostasis was evaluated during post-operative weeks 6-8 to avoid confounding by acute convalescence (Supplemental Figure 1C). Sham mice remained hyperglycemic and hyperinsulinemic compared to RYGB mice (Figure 2A). Glucose tolerance was improved after RYGB and glucose-stimulated plasma insulin reduced (Figure 2B, C). RYGB improved insulin sensitivity, as determined using HOMA-IR and insulin tolerance (Figure 2A, D). Liver triglyceride content was also reduced (8.9 ± 1.6 mg/g, RYGB vs. 113 ± 13 mg/g, Sham, $p < 0.05$). Comparable improvements occurred in CRWM-Sham mice (Figure 2).

To investigate which tissue(s) underlie this improved gluco-regulation, we used *in vivo* NMR metabolic flux analysis and 2-deoxy-glucose uptake to examine basal glucose production and peripheral glucose uptake, respectively. RYGB reduced *in vivo* hepatic glucose production, gluconeogenesis, and glycogenolysis (Figure 2E). In contrast, RYGB failed to enhance glucose uptake into skeletal muscle or adipose tissue (Supplemental Figure 2A). RYGB enhanced insulin-stimulated tyrosine phosphorylation of insulin receptor substrate-2 in the liver (Figure 2F), but not of insulin receptor substrate-1 in skeletal muscle (Supplemental Figure 2B). These effects were due, in part, to increased expression of IRS2 in the liver (Figure 2F). RYGB therefore improves glucose homeostasis via enhanced hepatic insulin signaling and sensitivity resulting in reduced glucose output.

MC4Rs are required for effects of RYGB on energy expenditure, body weight and glucose homeostasis

To determine the contribution of MC4R to these effects of RYGB, we studied MC4R-deficient (MC4R-null) and MC4R-heterozygous (MC4R-Het) mice, which harbor a loxP-modified null *Mc4r* allele whose expression is reactivated by Cre-recombinase.²⁰ Compared to a 31% reduction observed in DIO mice (Supplemental Figure 3), RYGB reduced the body weight of obese MC4R-null mice by only 10% (Figure 3A) due to its failure to increase energy expenditure (Figure 3B). The effect of RYGB to reduce fat mass was also attenuated (Supplemental Table 1). RYGB significantly reduced fasting blood glucose, but did not result in statistically-significant improvements in other measures of glucose homeostasis (Figure 4, left panels). These effects of RYGB were rescued in obese MC4R-Het mice (Figure 3C, D and Supplemental Table 1) demonstrating competency of one allele for mediating the MC4R-dependent effects of RYGB. Notably, RYGB reduced intake in these mice (Supplemental Table 1). Thus, RYGB induces an MC4R-dependent increase in energy expenditure to induce weight loss; MC4Rs are also required for improved glucose homeostasis after RYGB.

MC4Rs in cholinergic preganglionic vagal motor neurons mediate weight-independent effects of RYGB on glucose homeostasis

MC4Rs are expressed in key autonomic neurons including cholinergic preganglionic motor neurons of the parasympathetic dorsal motor vagus (DMV, i.e., vagal motor neurons) and of the sympathetic intermediolateral nucleus (IML)^{9-12, 14}. As reported by Rossi et al.,²¹ selective restoration of MC4Rs in autonomic brainstem neurons including cholinergic preganglionic neurons of the DMV (but not the IML) using Phox2b-Cre-mediated reactivation of expression in MC4R-null mice (Phox-MC4R) improves hyperinsulinemia linked to MC4R-deficiency but not hyperphagia, reduced energy expenditure, or obesity. In this study, we found that, HOMA-IR is improved in Phox-MC4R mice compared to MC4R-

null mice despite comparable obesity (Supplemental Figure 4A) reinforcing conclusions that MC4R-signaling via these cholinergic preganglionic neurons transmits weight-independent effects of MC4Rs on insulin sensitivity.

We therefore hypothesized that MC4Rs in cholinergic preganglionic neurons of the DMV mediate effects of RYGB on glucose homeostasis, but not body weight. Consistent with our hypothesis, RYGB in Phox-MC4R mice failed to increase energy expenditure and resulted in the same blunted weight reduction observed in MC4R-null mice (Figure 3A, B). RYGB also failed to reduce fat mass and food intake (Supplemental Table 1). As in MC4R-null mice, RYGB improved fasting glucose (Figure 4A). However, RYGB also improved fasting insulin, oral glucose tolerance, HOMA-IR, and insulin tolerance (Figure 4, B-F). Importantly, these improvements did not occur in MC4R-null mice, which exhibited the same blunted weight reduction after RYGB. RYGB did not reduce glucose-stimulated plasma insulin levels in Phox-MC4R mice (Figure 4E). However, liver triglycerides were reduced to a greater extent (67 ± 12 mg/g, RYGB vs. 162 ± 14 mg/g, Sham; $p < 0.05$) than in MC4R-null mice (115 ± 20 mg/g, RYGB vs. 218 ± 13 mg/g, Sham; $p < 0.05$). These data demonstrate that MC4Rs in cholinergic preganglionic motor neurons of the DMV mediate effects of RYGB on glucose and lipid homeostasis that are independent of changes in food intake, body composition, and body weight.

MC4Rs in cholinergic preganglionic neurons (sympathetic and parasympathetic) mediate effects of RYGB on energy expenditure and body weight

Prior work by Rossi, *et al.*,²¹ also demonstrated that restoration of MC4Rs in cholinergic preganglionic neurons of both the DMV and IML using ChAT-Cre-mediated re-activation of expression in MC4R-null mice (ChAT-MC4R), increases energy expenditure and attenuates obesity characteristic of MC4R deficiency. We therefore hypothesized that MC4R signaling in these neurons underlie effects of RYGB on energy expenditure and body weight. As MC4R is not re-activated in the IML of Phox-MC4R mice, these two complementary models enable direct comparison of events transmitted by MC4Rs in cholinergic preganglionic neurons of the IML (i.e., events occurring exclusively in ChAT-MC4R mice) versus those of the DMV (i.e., events occurring in Phox-MC4R mice).

Consistent with our hypothesis, RYGB-induced increased energy expenditure, reduced body weight, and reduced fat mass - responses that were absent in MC4R-null mice and Phox-Mc4R mice - were fully restored in ChAT-MC4R mice (Figure 3 and Supplemental Table 1). Food intake was also reduced (Supplemental Table 1). Fasting glucose and insulin, HOMA-IR, and glucose tolerance were all improved (Figure 4, A-D). In contrast to Phox-MC4R mice, glucose stimulated plasma insulin levels were reduced (Figure 4E). Liver triglycerides were not reduced in ChAT-MC4R mice (114 ± 17 mg/g, RYGB vs. 168 ± 26 mg/g, Sham; $p < 0.05$) compared to MC4R null mice (115 ± 20 mg/g, RYGB vs. 218 ± 13 mg/g, Sham; $p < 0.05$). Anti-diabetic effects occurring after RYGB in ChAT-MC4R mice were recapitulated in a separate group of sham-operated ChAT-MC4R control mice weight-matched to RYGB mice by calorie restriction (35.5 ± 1.3 g, RYGB vs. 36.8 ± 0.33 , CRWM-Sham; $p > 0.05$; Figure 4), as observed in DIO mice. Thus, MC4Rs in cholinergic preganglionic motor neurons of the IML, but not of the DMV, mediate RYGB-induced increased energy expenditure and reduced body weight; improved glucose homeostasis occurred as a secondary effect of weight loss.

RYGB improves hepatic glucose homeostasis in Phox-MC4R and ChAT-MC4R mice

We next compared effects of RYGB on pyruvate tolerance in Phox-MC4R and ChAT-MC4R mice. DIO mice were studied as a positive control. In DIO mice, RYGB reduced plasma glucose excursion after pyruvate administration (Supplemental Figure 4B)

suggesting reduced hepatic gluconeogenic capacity consistent with NMR metabolic flux results presented in Figure 2. Pyruvate-induced glucose excursion was also reduced in RYGB-treated ChAT-MC4R and Phox-MC4R mice (Supplemental Figure 4B) suggesting a similar hepatic mechanism as that occurring in DIO mice.

RYGB confers resistance to the weight-promoting effects of HFD

Stable weight reduction in RYGB-treated DIO mice despite equivalent intake compared to Sham suggests that RYGB confers resistance to HFD-induced weight gain. As C57BL/6 mice do not gain sufficient weight on regular chow to undergo RYGB, we addressed this hypothesis using obese MC4R-Het mice maintained on regular chow before and after surgery. These mice were then challenged with HFD for 8 days after post-operative weight stabilization, 8 weeks after surgery. As expected, Sham mice gained substantial weight on HFD (Figure 5A), consuming more energy at an increased efficiency (Figure 5B, C), consistent with their *Mc4r* haploinsufficiency. Their energy expenditure was reduced, likely as anabolic compensation for their weight gain (Figure 5D). In contrast, RYGB mice largely failed to gain weight on HFD (Figure 5A) despite a similar increase in consumption (Figure 5B), although overall intake remained reduced compared to Sham mice on HFD (65.0 ± 4.1 kJ/d, RYGB vs. 85.4 ± 2.7 kJ/d, Sham; $p < 0.05$). In contrast to Sham mice, metabolic efficiency was not increased in RYGB-treated mice on HFD (Figure 5C), suggesting a thermic effect of RYGB to prevent weight gain. This hypothesis was supported by their sustained, elevated energy expenditure (Figure 5D) compared to the reduction observed in Sham mice. Increased calorie losses did not account for this resistance to HFD (Supplemental Figure 5A). However, it did require MC4R as both RYGB and Sham MC4R-null mice, also maintained on regular chow, gained substantial and equivalent weight when challenged with HFD for 8 days (Figure 5A) or 3 weeks (Supplemental Figure 5B). RYGB therefore induces resistance to HFD-induced weight gain in an MC4R-dependent manner involving a blunted orexigenic response and increased energy expenditure.

Early diabetes remission after RYGB in carriers of the *MC4R*(I251L) variant

MC4R mutations comprise the most common forms of monogenic, early-onset obesity²² and non-synonymous coding variants occur in 1-6% of severely obese patients,¹⁷ yet carriers of these variants lose equivalent weight to non-carriers after RYGB.^{5, 18} However, we have demonstrated improved pre-surgery HOMA-IR and enhanced weight loss at 1 year after RYGB in carriers of *MC4R*(I251L),¹⁹ a variant associated with a decreased risk of obesity and increased basal receptor activity in cells,^{23, 24} suggestive of a mechanistic role for MC4R during RYGB. To investigate diabetes resolution after RYGB in carriers of rare *MC4R* variants, we sequenced the *MC4R* coding region in 1,433 patients undergoing RYGB and 451 age- and gender-matched lean patients. We found 18 patients with rare *MC4R* variants linked to obesity and 26 with I251L; no variants linked to obesity were found in the lean group while 1.6% carried I251L. Pre-operative BMI and metabolic profile for carriers and non-carriers were not different (Supplemental Figure 6 and Tables 2 and 3). We found that carriers of rare variants linked to obesity and non-carriers exhibited equivalent weight loss through 48 months of follow-up (Supplemental Figure 6). We then assessed diabetes remission in a paradigm comparable to those described by a consensus statement from the ADA.²⁵ Specifically, we used cessation of all anti-diabetic therapies 6 months post-surgery as an indication of remission. In individuals that fulfilled this criterion, we assessed cessation of anti-diabetic therapy 2 weeks post-RYGB. Despite minimal and equivalent post-surgical weight reduction (Figure 6A), 89% of I251L carriers (8 of 9 patients) no longer required diabetes medications by 2 weeks post-RYGB compared to only 66% of non-carriers (399 of 597 patients) and 50% of rare variant carriers (4 of 8 patients)(Figure 6B). These data show that RYGB confers weight-independent early diabetes remission in all

subjects and suggest that remission is improved in carriers of *MC4R(I251L)* compared to non-carriers.

Discussion

RYGB surgery provides the most effective, rapid, and long-lasting “cure” for type 2 diabetes. We show remission of type 2 diabetes in RYGB patients within 2 weeks after surgery with minimal weight loss. Interestingly, one competent allele of *MC4R* is sufficient for diabetes remission and long-term weight loss, while the common *I251L* allele, associated with better metabolic profile and enhanced basal receptor activity in cells, seems to accelerate early diabetes remission. To gain insight into the mechanism of diabetes resolution and a specific role for *MC4R*, we use mouse models where RYGB improves glucose homeostasis independent of changes in food intake, body composition, and body weight.

We find that in Phox-MC4R mice with selective MC4R reactivation in cholinergic preganglionic neurons of the DMV, RYGB improves glucose and lipid homeostasis despite ongoing hyperphagia and obesity. Improved glucose and lipid homeostasis occurring after RYGB in these mice is well beyond that observed in MC4R-null mice, which exhibit the same blunted weight loss (8 vs. 10%, respectively) and reduced fat mass after RYGB. In fact, they are equivalent in magnitude to those occurring in DIO and ChAT-MC4R mice, which exhibit substantially greater weight loss after RYGB (~27-31%). As these effects do not occur in similarly obese and hyperphagic RYGB-treated MC4R-null mice, they are therefore independent of changes in body weight, body composition, energy expenditure, and food intake. Notably, glucose homeostasis was improved in these reactivation mice as compared to their respective Sham controls but not as compared to lean, insulin-sensitive mice, precluding determination of diabetes “resolution.”

In contrast, MC4Rs in both parasympathetic (i.e., DMV) and sympathetic (i.e., IML) cholinergic preganglionic neurons transduce effects of RYGB on energy expenditure and body weight, as determined using ChAT-MC4R mice. We conclude that MC4Rs of the IML are responsible for these energetic and body weight effects as RYGB fails to increase energy expenditure and induce substantial weight loss in Phox-MC4R mice, mice in which MC4Rs are restored in the DMV, but not in the IML. That RYGB induces beneficial effects in Phox-MC4R and ChAT-MC4R mice greater than MC4R reactivation alone suggests that RYGB enhances MC4R activity in these neurons to mediate its effects.

In DIO mice, we find that RYGB enhances insulin sensitivity to reduce hepatic glucose output. As suggested by pyruvate tolerance, RYGB induces similar reduced hepatic gluconeogenesis in Phox-MC4R and ChAT-MC4R mice as it does in DIO mice. However, the mechanism is different. In ChAT-MC4R mice, recapitulation of all RYGB-induced anti-diabetic effects in CRWM-Sham controls suggests that glucose homeostasis is improved predominately as a consequence of weight loss. In contrast, the failure of RYGB to reduce glucose stimulated plasma insulin in Phox-MC4R mice suggests a neuronal mechanism converging on the liver to reduce glucose output, consistent with the selective MC4R reactivation in the DMV of these mice. A gut-brain-liver circuit regulating hepatic glucose production via the vagus nerve is well-recognized.²⁶ We propose that RYGB improves hepatic insulin signaling via enhanced MC4R activity in vagal motor neurons, which reduces hepatic steatosis and results in secondary improvements of glucose homeostasis. Such a mechanism could explain improved glycemia prior to post-surgical weight loss and early anti-diabetic effects of RYGB resulting from hepatic sensitization in humans.²⁷⁻²⁹ Unresolved issues include exactly how the MC4R pathway is engaged following RYGB. Secretion of gut hormones, many of which modulate MC4R function, is augmented after

RYGB³⁰ and MC4R-expressing hindbrain nuclei receive afferent innervations from the gut and other abdominal viscera. However, the identity of gut-derived afferent signals involved in the MC4R-dependent effects of RYGB is currently unclear but of obvious relevance to fully elucidating the mechanisms of RYGB.

Our mouse model reproduces beneficial effects of RYGB on body weight, body composition, stool energy, and glucose homeostasis observed in humans.³¹⁻³³ This is likely because our surgical model closely mimics gastric manipulation and intestinal bypass as they occur in the human procedure. In contrast, other surgical models previously studied in genetically-manipulated mice utilize anatomical manipulations that do not achieve gastric bypass and are not used as bariatric procedures in humans,^{34, 35} limiting their applicability to mechanisms of human RYGB. Conclusions from these studies are additionally limited by experiments performed at early post-operative time points (i.e., 10 days), which are confounded by acute post-operative convalescence,^{34, 35} and the lack of *ad libitum*-fed Sham controls for post-operative stress.³⁴

An apparent divergence of our model from human RYGB is the failure to reduce intake in DIO mice. However, DIO in C57BL/6 mice is primarily metabolic (i.e., due to increased feeding efficiency), rather than due to hyperphagia³⁶⁻⁴¹. For example, male C57BL/6 mice can become obese on HFD despite equivalent calorie intake as control mice on regular chow^{36, 38} and gain more weight than other diet-sensitive strains consuming equivalent calories on HFD^{37, 38}. Therefore, RYGB seems to reverse the primary metabolic disorder resulting in the obesity of DIO C57BL/6 mice, without affecting intake. In contrast, hyperphagia contributes substantially to the obesity of MC4R-deficiency, and intake is reduced in ChAT-MC4R and MC4R-Het mice after RYGB. In addition, RYGB reduces intake in other hyperphagic mouse models of obesity we have tested (data not shown). Thus, our model is competent to reduce intake, a hallmark of the human procedure, and the lack of effect in DIO C57BL/6 mice is a limitation of the DIO model itself.

Similarly, dysglycemia in DIO C57BL/6 mice is predominately the result of elevated hepatic glucose production rather than reduced peripheral uptake.⁴⁰ Thus, the predominant hepatic effect we observed may also be due to innate characteristics of the DIO C57BL/6 model, explaining the apparent discrepancy with increased uptake observed after RYGB in patients.⁴² However, equivalent glucose uptake despite substantially reduced basal and stimulated plasma insulin compared to Sham mice suggests that glucose uptake may actually be increased after RYGB. While this could be clarified using insulin clamp technology, this methodology is beyond the scope of the manuscript and would still be confounded by the substantial reductions in body weight, fat mass, and lean mass observed after RYGB.

The effect of RYGB on energy expenditure represents ~10% of daily energy intake. It is slightly less than the calorie restriction required to induce comparable weight reduction in CRWM-Sham mice demonstrating the magnitude of anabolic compensation occurring in CRWM-Sham mice and catabolism induced by RYGB. Thus, RYGB mice remain catabolic despite sustained and substantial weight loss as well as a reduction in leptin capable of inducing a compensatory anabolic response in CRWM-Sham mice. This suggests enhanced leptin sensitivity and defense of a lower body weight after RYGB. In addition, RYGB-treated MC4R-Het, but not MC4R-null, mice resist HFD-induced positive energy balance and weight gain further suggesting defense of a lower body weight after RYGB as well as plasticity of the RYGB-induced thermogenic response based on energetic needs. These findings are incompatible with an anatomic mechanism of weight loss, which would induce a compensatory anabolic response as seen in CRWM-Sham mice. Instead, they suggest that RYGB induces a new steady-state of energy homeostasis at a lower body weight via MC4Rs.

In summary, we demonstrate neuronal mechanisms whereby effects of RYGB on glucose homeostasis diverge from its effects on energy expenditure and body weight. MC4Rs in cholinergic preganglionic vagal motor neurons transmit effects of RYGB on glucose and lipid homeostasis independent of changes in food intake, body composition, and body weight. In contrast, MC4Rs in cholinergic preganglionic neurons of the sympathetic IML transmit effects of RYGB on energy expenditure and body weight. Our findings suggest neuronally-mediated enhanced insulin signaling in the liver also mediates a reduction in glucose output and resolution of hepatic steatosis. This mechanism likely explains early, weight-independent effects of RYGB on diabetes in humans. In support of this hypothesis, carriers of the *MC4R*(I251L) variant exhibit enhanced early diabetes resolution after surgery that is weight-independent compared to non-carriers. Thus, MC4Rs coordinate an efferent autonomic mechanism utilized by RYGB to induce its beneficial effects in mice and humans.

Methods

Animals

Studies were conducted in accordance with UT Southwestern Institutional Animal Care and Use Committee and the Association of Assessment and Accreditation of Laboratory Animal Care policies. Where specified, animals were provided rodent chow (2016, Teklad) or HFD (D12492, Research Diets). *LoxTB-MC4R* (MC4R-null) and *ChAT-cre, loxTB-MC4R* (*ChAT-MC4R*) were a kind gift from Brad Lowell; *Phox2b-cre, loxTB-MC4R* (*Phox-MC4R*) mice were generated as described.^{20, 21} All mouse models were back-crossed (at least 8 generations) into a pure C57BL/6 background.

Surgery

RYGB involved gastrointestinal reconstruction connecting a restricted proximal gastric pouch to a jejunal afferent limb (Supplemental Figure 1D). The proximal gut was excluded from alimentary flow using a hemostasis clip (Ethicon) placed just distal to the gastro-jejunosomy. Sham procedure involved gastrotomy, enterotomy, and repair. Anesthesia was provided using a scavenged circuit of isoflurane and anesthesia time standardized between groups. Mice were maintained on a standardized post-operative protocol during which liquid diet was provided from post-operative day 2-7. On post-operative day 6, 0.25g of HFD was provided on a daily basis until consumed in its entirety. Subsequently, solid diet was re-introduced *ad libitum*.

Study design

C57BL/6 males were maintained on HFD diet from 6 weeks of age; MC4R models on regular chow from weaning. Upon reaching 50g (12-14 weeks on HFD for DIO; 18-22 weeks of age for MC4R models), mice were randomized to RYGB or sham operations. A subset of sham-operated DIO and *ChAT-MC4R* mice were weight-matched to their RYGB counterparts by calorie restriction (CRWM-Sham). After post-operative recovery, mice were provided HFD (DIO) or regular chow (genetically-modified mice) *ad libitum*. Body composition was evaluated using a Minispec mq10 NMR (Bruker Optics). Food intake was measured over 4 consecutive days during week 4, unless otherwise noted. Physical activity was measured in metabolic cages during week 5 (TSE Systems GmbH). Glucose homeostasis, including *in vivo* NMR metabolic flux and insulin signaling, was evaluated during weeks 6-8. Animals were sacrificed during week 8.

Supplementary Material

Refer to Web version on PubMed Central for supplementary material.

Acknowledgments

Grant Support: This work was supported by funds from UT Southwestern Department of Medicine and DK091511 (VA); from the Geisinger Clinic, the Weis Center for Research, the Geisinger Obesity Research Institute (TM, GSG, and CDS); from DK072488 and DK088231 (GSG and CDS); from DK092775 (TM); and, from DK078184 (SB).

References

- Schauer PR, Burguera B, Ikramuddin S, et al. Effect of laparoscopic Roux-en Y gastric bypass on type 2 diabetes mellitus. *Ann Surg.* 2003; 238:467–84. discussion 84-5. [PubMed: 14530719]
- Wickremesekera K, Miller G, Naotunne TD, et al. Loss of insulin resistance after Roux-en-Y gastric bypass surgery: a time course study. *Obes Surg.* 2005; 15:474–481. [PubMed: 15946424]
- Scott WR, Batterham RL. Roux-en-Y gastric bypass and laparoscopic sleeve gastrectomy: understanding weight loss and improvements in type 2 diabetes after bariatric surgery. *Am J Physiol Regul Integr Comp Physiol.* 2011; 301:R15–27. [PubMed: 21474429]
- Nestoridi E, Kvas S, Kucharczyk J, et al. Resting Energy Expenditure and Energetic Cost of Feeding Are Augmented after Roux-en-Y Gastric Bypass in Obese Mice. *Endocrinology.* 2012; 153:2234–44. [PubMed: 22416083]
- Hatoum II, Stylopoulos N, Vanhoose AM, et al. Melanocortin-4 Receptor Signaling Is Required for Weight Loss after Gastric Bypass Surgery. *J Clin Endocrinol Metab.* 2012; 97
- Huszar D, Lynch CA, Fairchild-Huntress V, et al. Targeted disruption of the melanocortin-4 receptor results in obesity in mice. *Cell.* 1997; 88:131–141. [PubMed: 9019399]
- Vaisse C, Clement K, Guy-Grand B, et al. A frameshift mutation in human MC4R is associated with a dominant form of obesity. *Nat Genet.* 1998; 20:113–4. [PubMed: 9771699]
- Yeo GS, Farooqi IS, Aminian S, et al. A frameshift mutation in MC4R associated with dominantly inherited human obesity. *Nat Genet.* 1998; 20:111–2. [PubMed: 9771698]
- Kishi T, Aschkenasi CJ, Lee CE, et al. Expression of melanocortin 4 receptor mRNA in the central nervous system of the rat. *J Comp Neurol.* 2003; 457:213–235. [PubMed: 12541307]
- Liu H, Kishi T, Roseberry AG, et al. Transgenic mice expressing green fluorescent protein under the control of the melanocortin-4 receptor promoter. *J Neurosci.* 2003; 23:7143–54. [PubMed: 12904474]
- Mountjoy KG, Mortrud MT, Low MJ, et al. Localization of the melanocortin-4 receptor (MC4-R) in neuroendocrine and autonomic control circuits in the brain. *Mol Endocrinol.* 1994; 8:1298–308. [PubMed: 7854347]
- Song CK, Jackson RM, Harris RB, et al. Melanocortin-4 receptor mRNA is expressed in sympathetic nervous system outflow neurons to white adipose tissue. *Am J Physiol Regul Integr Comp Physiol.* 2005; 289:R1467–76. [PubMed: 16221982]
- Ellacott KL, Cone RD. The central melanocortin system and the integration of short- and long-term regulators of energy homeostasis. *Recent Prog Horm Res.* 2004; 59:395–408. [PubMed: 14749511]
- Voss-Andreae A, Murphy JG, Ellacott KL, et al. Role of the central melanocortin circuitry in adaptive thermogenesis of brown adipose tissue. *Endocrinology.* 2007; 148:1550–1560. [PubMed: 17194736]
- Wan S, Browning KN, Coleman FH, et al. Presynaptic melanocortin-4 receptors on vagal afferent fibers modulate the excitability of rat nucleus tractus solitarius neurons. *J Neurosci.* 2008; 28:4957–4966. [PubMed: 18463249]
- Gautron L, Lee C, Funahashi H, et al. Melanocortin-4 receptor expression in a vago-vagal circuitry involved in postprandial functions. *J Comp Neurol.* 2010; 518:6–24. [PubMed: 19882715]
- Lubrano-Berthelier C, Dubern B, Lacorte JM, et al. Melanocortin 4 receptor mutations in a large cohort of severely obese adults: prevalence, functional classification, genotype-phenotype relationship, and lack of association with binge eating. *J Clin Endocrinol Metab.* 2006; 91:1811–8. [PubMed: 16507637]

18. Aslan IR, Campos GM, Calton MA, et al. Weight Loss after Roux-en-Y Gastric Bypass in Obese Patients Heterozygous for MC4R Mutations. *Obes Surg.* 2010; 21:930–4. [PubMed: 20957447]
19. Mirshahi UL, Still CD, Masker KK, et al. The MC4R(I251L) allele is associated with better metabolic status and more weight loss after gastric bypass surgery. *J Clin Endocrinol Metab.* 2011; 96:E2088–96. [PubMed: 21976721]
20. Balthasar N, Dalgaard LT, Lee CE, et al. Divergence of melanocortin pathways in the control of food intake and energy expenditure. *Cell.* 2005; 123:493–505. [PubMed: 16269339]
21. Rossi J, Balthasar N, Olson D, et al. Melanocortin-4 receptors expressed by cholinergic neurons regulate energy balance and glucose homeostasis. *Cell Metab.* 2011; 13:195–204. [PubMed: 21284986]
22. Loos RJ. The genetic epidemiology of melanocortin 4 receptor variants. *Eur J Pharmacol.* 2011; 660:156–64. [PubMed: 21295023]
23. Xiang Z, Litherland SA, Sorensen NB, et al. Pharmacological characterization of 40 human melanocortin-4 receptor polymorphisms with the endogenous proopiomelanocortin-derived agonists and the agouti-related protein (AGRP) antagonist. *Biochemistry.* 2006; 45:7277–88. [PubMed: 16752916]
24. Stutzmann F, Vatin V, Cauchi S, et al. Non-synonymous polymorphisms in melanocortin-4 receptor protect against obesity: the two facets of a Janus obesity gene. *Hum Mol Genet.* 2007; 16:1837–44. [PubMed: 17519222]
25. Buse JB, Caprio S, Cefalu WT, et al. How do we define cure of diabetes? *Diabetes Care.* 2009; 32:2133–5. [PubMed: 19875608]
26. Lam CK, Chari M, Lam TK. CNS regulation of glucose homeostasis. *Physiology (Bethesda).* 2009; 24:159–170. [PubMed: 19509126]
27. Promintzer-Schifferl M, Prager G, Anderwald C, et al. Effects of gastric bypass surgery on insulin resistance and insulin secretion in nondiabetic obese patients. *Obesity (Silver Spring).* 2011; 19:1420–6. [PubMed: 21494227]
28. Lima MM, Pareja JC, Alegre SM, et al. Acute effect of roux-en-y gastric bypass on whole-body insulin sensitivity: a study with the euglycemic-hyperinsulinemic clamp. *J Clin Endocrinol Metab.* 2010; 95:3871–3875. [PubMed: 20484482]
29. Klein S, Mittendorfer B, Eagon JC, et al. Gastric bypass surgery improves metabolic and hepatic abnormalities associated with nonalcoholic fatty liver disease. *Gastroenterology.* 2006; 130:1564–1572. [PubMed: 16697719]
30. Cummings DE. Endocrine mechanisms mediating remission of diabetes after gastric bypass surgery. *Int J Obes (Lond).* 2009; 33(1):S33–40. [PubMed: 19363506]
31. Buchwald H, Estok R, Fahrbach K, et al. Weight and type 2 diabetes after bariatric surgery: systematic review and meta-analysis. *Am J Med.* 2009; 122:248–256. e5. [PubMed: 19272486]
32. Chaston TB, Dixon JB, O'Brien PE. Changes in fat-free mass during significant weight loss: a systematic review. *Int J Obes (Lond).* 2007; 31:743–50. [PubMed: 17075583]
33. Odstrcil EA, Martinez JG, Santa Ana CA, et al. The contribution of malabsorption to the reduction in net energy absorption after long-limb Roux-en-Y gastric bypass. *Am J Clin Nutr.* 2010; 92:704–713. [PubMed: 20739420]
34. Troy S, Soty M, Ribeiro L, et al. Intestinal gluconeogenesis is a key factor for early metabolic changes after gastric bypass but not after gastric lap-band in mice. *Cell Metab.* 2008; 8:201–211. [PubMed: 18762021]
35. Chandarana K, Gelegen C, Karra E, et al. Diet and gastrointestinal bypass-induced weight loss: the roles of ghrelin and peptide YY. *Diabetes.* 2011; 60:810–818. [PubMed: 21292870]
36. West DB, Boozer CN, Moody DL, et al. Dietary obesity in nine inbred mouse strains. *Am J Physiol.* 1992; 262:R1025–r1032. [PubMed: 1621856]
37. Surwit RS, Feinglos MN, Rodin J, et al. Differential effects of fat and sucrose on the development of obesity and diabetes in C57BL/6J and A/J mice. *Metabolism.* 1995; 44:645–51. [PubMed: 7752914]
38. Brownlow BS, Petro A, Feinglos MN, et al. The role of motor activity in diet-induced obesity in C57BL/6J mice. *Physiol Behav.* 1996; 60:37–41. [PubMed: 8804640]

39. Parekh PI, Petro AE, Tiller JM, et al. Reversal of diet-induced obesity and diabetes in C57BL/6J mice. *Metabolism*. 1998; 47:1089–1096. [PubMed: 9751238]
40. Rossmeisl M, Rim JS, Koza RA, et al. Variation in type 2 diabetes--related traits in mouse strains susceptible to diet-induced obesity. *Diabetes*. 2003; 52:1958–1966. [PubMed: 12882911]
41. Petro AE, Cotter J, Cooper DA, et al. Fat, carbohydrate, and calories in the development of diabetes and obesity in the C57BL/6J mouse. *Metabolism*. 2004; 53:454–457. [PubMed: 15045691]
42. Gregor MF, Yang L, Fabbrini E, et al. Endoplasmic reticulum stress is reduced in tissues of obese subjects after weight loss. *Diabetes*. 2009; 58:693–700. [PubMed: 19066313]

Abbreviations

RYGB	Roux-en-Y gastric bypass
MC4R	melanocortin-4 receptor
DIO	diet-induced obesity
CRWM-Sham	calorie-restricted, weight-matched Sham
HFD	high fat diet
DMV	dorsal motor vagus
IML	intermediolateral nucleus

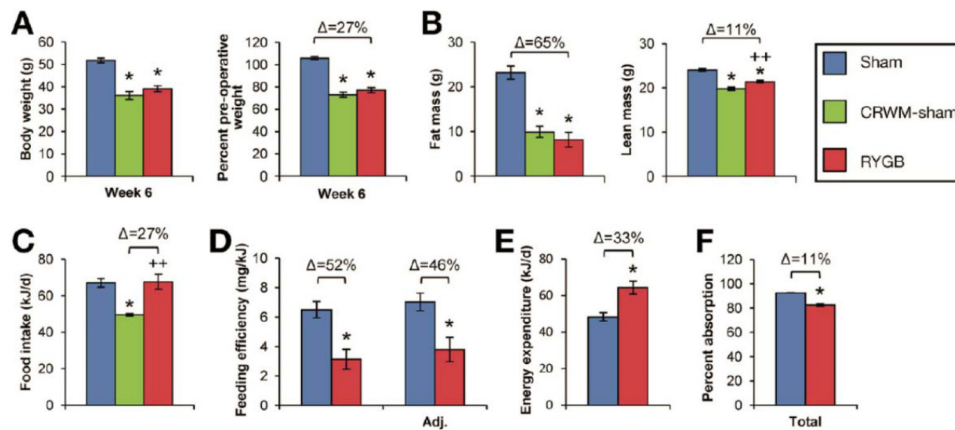


Figure 1. RYGB induces weight loss in DIO mice

(A) Total body weight (left) during post-operative week 6 and expressed as a percentage of pre-operative weight (right) in RYGB-treated (red), Sham (blue), and calorie-restricted, weight-matched Sham mice (CRWM-Sham, in green) (n=27, RYGB; n=29, Sham; n=12, CRWM-Sham). (B) Reduced fat and lean mass in RYGB and CRWM-Sham mice (n=4/group). (C) RYGB did not reduce food intake (n=11-25/group). Daily calorie restriction required to weight-match CRWM-Sham mice (n=12) to RYGB mice is shown in green. (D) RYGB reduced feeding efficiency (weight gain per kJ consumed). Feeding efficiency remained substantially reduced after adjusting for fecal energy losses (Adj. feeding efficiency)(n=11-25/group). (E) Energy expenditure was increased by 33% after RYGB (n=11-25/group). (F) Calorie absorption was slightly reduced after RYGB (n=8/group). * $p < .05$ vs. Sham, ** $p < .05$ vs. CRWM-Sham.

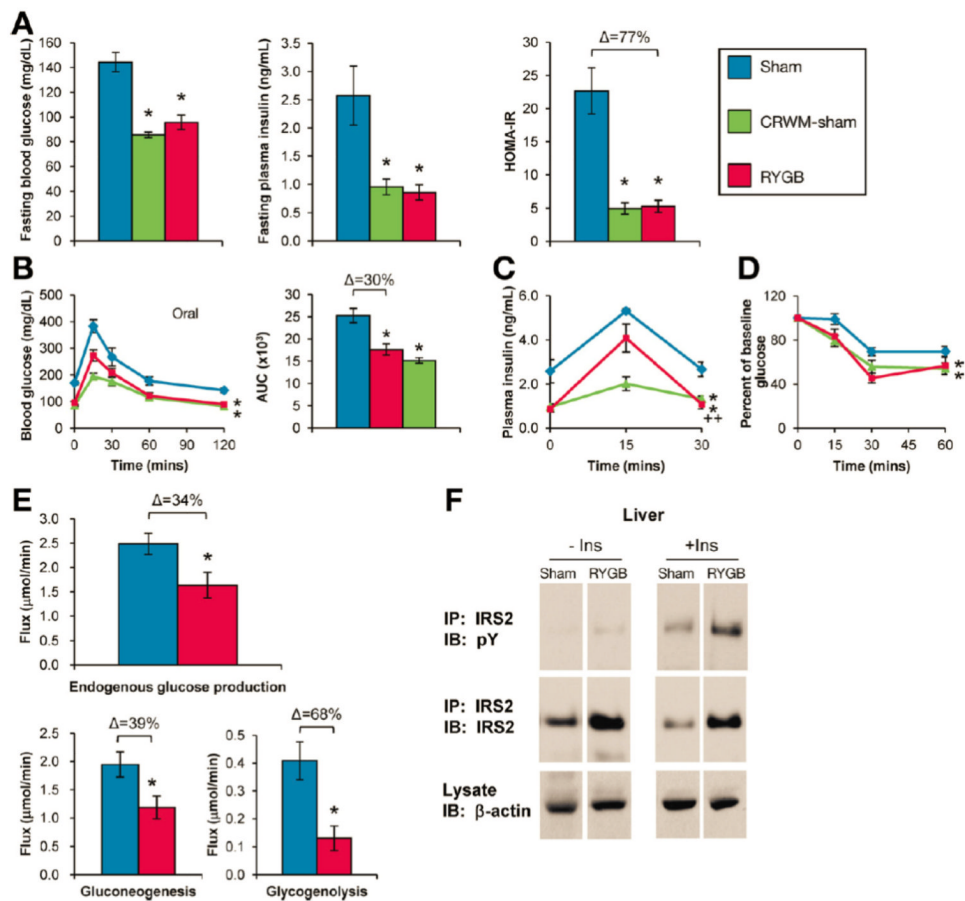


Figure 2. RYGB improves hepatic glucose homeostasis in DIO mice

(A) RYGB reduced fasting glucose (left), fasting insulin (middle), and HOMA-IR (right) ($n=4-11/\text{group}$). (B) RYGB improved oral glucose tolerance, (C) reduced glucose-stimulated plasma insulin, and (D) improved insulin tolerance, presented as % of baseline glucose to control for differences in baseline glucose ($n=5-6/\text{group}$). (E) RYGB reduced basal endogenous glucose production, gluconeogenesis, and glycogenolysis as measured during week 6 using *in vivo* NMR metabolic flux analysis ($n=5-9/\text{group}$). (F) RYGB increased insulin-stimulated IRS2 tyrosine phosphorylation and protein expression ($n=4/\text{group}$). IP, immunoprecipitate; IB, immunoblot. * $p<.05$ vs. Sham, ** $p<.05$ vs. CRWM-Sham.

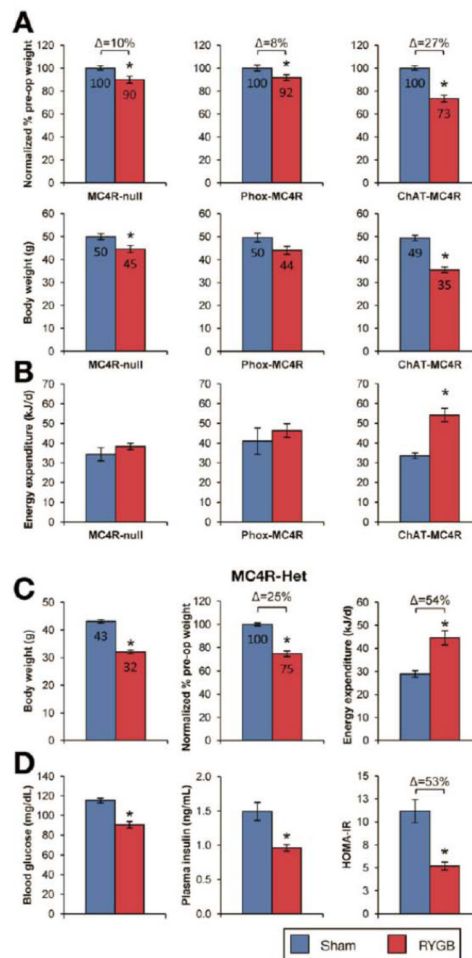


Figure 3. MC4Rs in autonomic neurons mediate effects of RYGB on energy expenditure and body weight

(A) RYGB-induced weight loss was attenuated in both MC4R-null (left) and Phox-MC4R mice (middle). In contrast, RYGB induced substantial weight reduction in ChAT-MC4R mice (right). The weight reduction observed in ChAT-MC4R mice was comparable to that seen in DIO mice (See Supplemental Figure 3). Body weight is presented as total (bottom) and also expressed as percentage of pre-operative weight (top), to facilitate comparison of the relative effects of RYGB across genotypes ($n=22-24/\text{group}$, MC4R-null; $n=6-22/\text{group}$, Phox-MC4R and ChAT-MC4R). (B) RYGB failed to increase energy expenditure in MC4R-null and Phox-MC4R mice ($n=10-25/\text{group}$, MC4R-null; $n=6-22/\text{group}$, Phox-MC4R). In contrast, RYGB increased energy expenditure in ChAT-MC4R mice, consistent with their weight loss ($n=6-22/\text{group}$, ChAT-MC4R mice). (C) RYGB reduced body weight of obese MC4R-Het mice by 25% during week 6 ($n=7-10/\text{group}$). Consistent with their weight reduction after RYGB, energy expenditure was increased in MC4R-Het mice ($n=7-10$). (D) RYGB improved fasting glucose, fasting insulin, and HOMA-IR in MC4R-Het mice ($n=7-10$). * $p < .05$ vs. Sham.

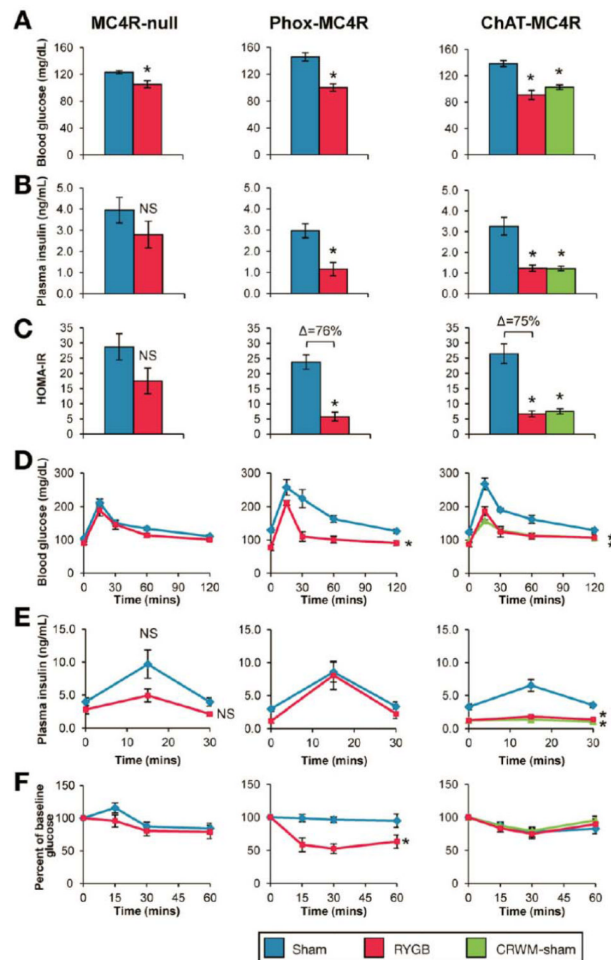


Figure 4. MC4Rs in parasympathetic vagal motor neurons mediate effects of RYGB on glucose homeostasis independent of changes in body weight

(A-F, left panels) RYGB significantly reduced fasting glucose in MC4R-null mice, but failed to produce statistically-significant improvements in other measures of glucose homeostasis: insulin (B), HOMA-IR (C), glucose tolerance (D), glucose-stimulated plasma insulin (E), and insulin tolerance (F), presented as % of baseline glucose to control for differences in baseline glucose (n=6-14/group). (A-F, middle panels) In contrast, RYGB reduced fasting glucose (A) and insulin (B), and improved HOMA-IR (C), oral glucose tolerance (D), and insulin tolerance (F) in Phox-MC4R mice, despite a similar blunted weight-reduction as seen in MC4R-null mice. RYGB did not reduce their glucose-stimulated plasma insulin (n=6-7/group). (A-F, right panels) Consistent with their substantial weight reduction, fasting glucose (A), fasting plasma insulin (B), and glucose-stimulated plasma insulin (C) were reduced and oral glucose tolerance improved (D) in RYGB-treated ChAT-MC4R mice and CRWM-Sham ChAT-MC4R mice (n=6-7/group). * $p < .05$ vs. Sham.

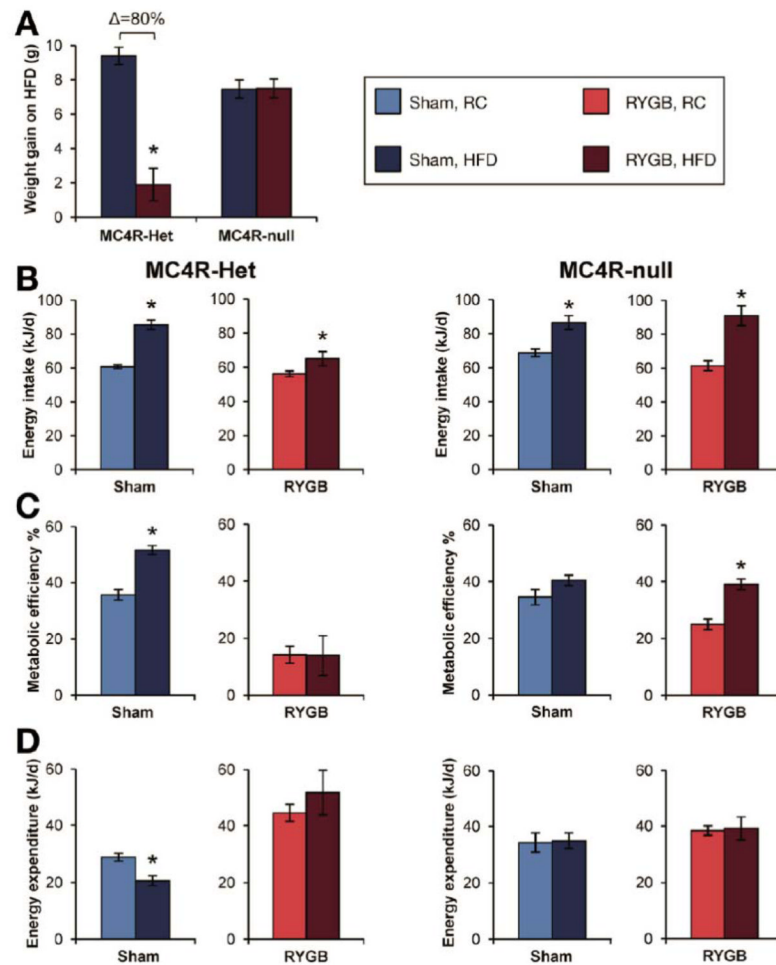


Figure 5. RYGB induces resistance to HFD-induced weight-gain

(A) RYGB-treated MC4R-Het mice fail to gain weight upon challenge with HFD for 8 days compared to Sham mice. In contrast, Sham- and RYGB-treated MC4R-null mice gained substantial and equivalent weight ($n=4-11/\text{group}$) (B) Food intake was increased on HFD in RYGB-treated and Sham-operated mice of both genotypes ($n=4-11/\text{group}$). (C and D) Sham-operated MC4R-Het and MC4R-null mice and RYGB-treated MC4R-null mice assimilate all excess consumed energy on HFD as body mass at an elevated metabolic efficiency. Energy expenditure is reduced in Sham-operated MC4R-Het mice as a compensation for their weight gain on HFD. In contrast, RYGB-treated MC4R-Het mice fail to increase their metabolic efficiency on HFD. In addition, their elevated energy expenditure persists and remains elevated versus Sham MC4R-Het mice ($n=4-11/\text{group}$). * $p<.05$ RYGB vs. Sham or HFD vs. RC.

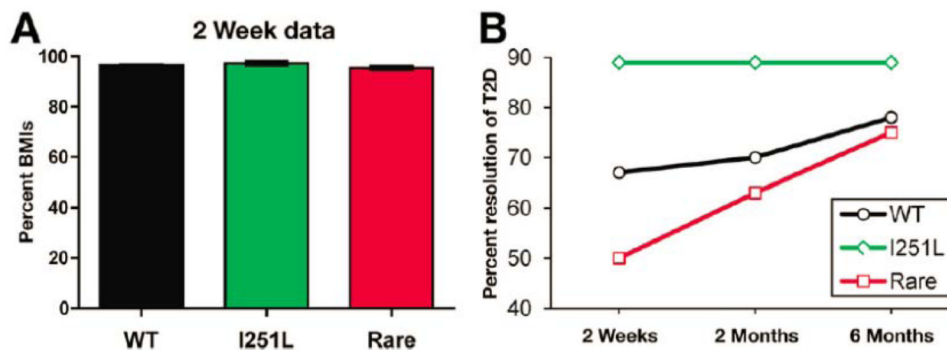


Figure 6. MC4Rs mediate beneficial effects of RYGB on glucose homeostasis in humans with rare *MC4R* variants

(A) Post-operative weight, expressed as a percentage of pre-operative BMI (%BMIs), was equivalent in *MC4R(I251L)* carriers (green; n=26), rare variant carriers linked to obesity (red; n=18) and non-carriers (black; n=1399) at two weeks post-operative (range 10-20 days). (B) Resolution of type 2 diabetes (T2D), defined as cessation of all anti-diabetic medications, in carriers of the *MC4R(I251L)* variant (green; 8 of 9 patients), carriers of rare *MC4R* variants (red; 4 of 8) and non-carriers (black; 399 of 597) at 2 weeks, 2 months, and 6 months after RYGB.